JOURNAL OF GEOPHYSICAL RESEARCH, VOL. 91, NO. B11, PAGES 11,477-11,495, OCTOBER 10, 1986

CONSORTIUM FOR CONTINENTAL REFLECTION PROFILING MICHIGAN SURVEYS: REPROCESSING AND RESULTS

Tianfei Zhu[1] and Larry D. Brown

Institute for the Study of the Continents and Department of Geological Sciences
Cornell University, Ithaca, New York

Abstract. Reprocessing of Consortium for Continental Reflection Profiling data from central Michigan, with emphasis on deconvolution and velocity filtering before stack and more detailed velocity analysis, has resulted in greatly improved imaging of a previously reported Keweenawan rift buried beneath the Paleozoic of the Michigan Basin. The seismic stratigraphy of the sub-Paleozoic units can now be related to the basin-filling Middle Keweenawan volcanic sequence and the Upper Keweenawan clastic assemblage in greater detail. Important structural and stratigraphic features can be seen for the first time. For example, reprocessing has imaged an unconformity within the Upper Keweenawan. It is possible some of these newly imaged features are associated with a late Keweenawan compressive episode. Furthermore, reprocessing also reveals previously unrecognized sub-Keweenawan structures, including a deeply penetrating reflection which may represent a major crustal fault, and possible weak reflections from midcrustal (25 km) and Moho (43 km) depths.

Introduction

The Michigan Basin is an intracratonic basin with a near-circular geometry (Figure 1). As the basin has been actively explored for oil and gas over the past 40 years, its Phanerozoic geologic history is well documented [Sleep and Sloss, 1978]. Paleozoic subsidence started in Middle or Late Cambrian time with the deposition of Cambrian to Middle Ordovician sediments in a southward deepening embayment [Catacosinos, 1973]. However, the basin began to take on its present geometry in Middle Ordovician time. The sedimentary units accumulating during this period generally thicken toward the basin center near Saginaw Bay, where the maximum depth to the Precambrian basement exceeds 4.5 km (Figure 1) [Hinze et al., 1975]. The cause of this subsidence has long been of interest to geologists. Early and recent works were respectively summarized by Ells [1969] and Sleep and Sloss [1978]. While Hinze and Merritt [1969] and Craddock [1972] associated the subsidence with the Keweenawan structure beneath the basin, more recently proposed models have related post-Early Ordovician subsidence to deep-seated processes such as thermal contraction, lower crustal phase changes, and diapiric injections into the lithosphere [e.g., Sleep and Snell, 1976; Haxby et al., 1976; Nunn and Sleep, 1984]. However, there seems to be no independent evidence in the geologic record to substantiate such thermal events. Furthermore, in order to explain the entire Paleozoic subsidence history with a thermal model, multiple heating events are required [Sleep and Sloss, 1978].

Transecting the Michigan Basin from northwest to southeast are a prominent positive gravity anomaly (mid-Michigan gravity high) (Figure 2) and an associated but less well-defined positive magnetic anomaly. By analogy to the Midcontinent Geophysical Anomaly (MGA) (Figure 2) and by tracing theanomalies to Precambrain exposures near Lake Superior, these anomalies have generally been interpreted as representing a buried rift of Keweenawan age beneath the basin [e.g., Hinze et al., 1975].

In 1978, Consortium for Continental Reflection Profiling (COCORP) surveyed three deep Vibroseis (TM Continental Oil Company) reflection profiles across the mid-Michigan gravity high near the McClure-Sparks No. 1-8 deep well (Figure 1). Initial results from these surveys were reported by Brown et al. [1982]. Although the quality of the original seismic sections was generally poor, three distinct reflection units were identified (Figure 3). An upper 1.5 s of flat-lying reflections were associated with the Paleozoic strata. A reflection-poor zone from about 1.5 to 3.0 s was inferred to correspond to an underlying Upper Keweenawan clastic assemblage. Most importantly, a sequence of relatively prominent reflections from about 8 km (3.0 s) to 14 km (5.0 s) defines a structural trough and was interpreted as a Middle Keweenawan volcanic sequence [Brown et al., 1982]. Unfortunately, reflections from these units are poorly defined on the original sections, and the poor data quality tended to obscure potentially important structural and stratigraphic details, particularly in the lowest unit. With very few exceptions, no structures deeper than 14 km were evident on the original seismic sections (Figure 3).

The Michgan surveys were carried out relatively early in COCORP's history, well before COCORP had its own processing facility. At that time, processing was performed by a contractor within relatively narrow bounds. The need for more extensive processing and the desire to inject more geologic guidance into the processing sequence were driving forces behind COCORP's move to take over its own processing. The degree and type of processing now routinely accorded new COCORP data are greatly evolved from the basic treatments which cored the early experiments.

The Michigan data were reprocessed in this study in a manner more representive of current COCORP procedures. This study was spurred by the COCORP Kansas survey at the southern end of the MGA (Figure 2), which found a remarkably similar Keweenawan seismic stratigraphy as well as many deep structures not at all evident in the original Michigan results [Serpa et al., 1984].

[1]Now at Tennessee Earthquake Information Center, Memphis State University, Memphis.

Paper number 6B6033.
0148-0227/86/006B-6033$05.00

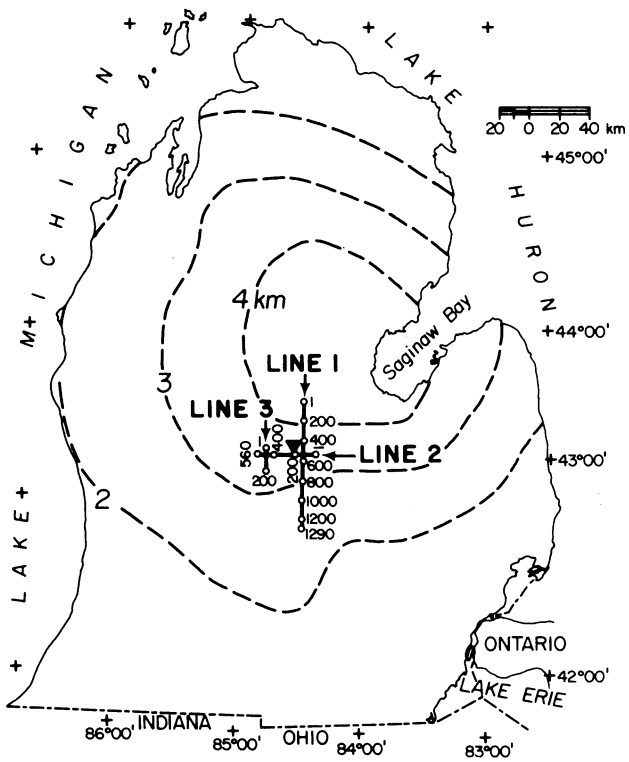

Fig. 1. Depth to basement within the Michigan Basin with the location of COCORP seismic lines 1 (87 km), 2 (38 km), and 3 (13 km). Numbers refer to vibration points (VPs), spaced 67 m apart. Location of the McClure-Sparks No. 1-8 deep well indicated by triangle [from Brown et al., 1982].

The reprocessing of the Michigan data has produced significantly improved seismic sections which not only provide a firm basis for refining and expanding the original interpretation of the Keweenawan stratigraphy but also image deeper crustal structures not apparent to the earlier treatments.

Seismic Noise

COCORP employs the same data processing techniques as the petroleum industry for generating a stacked section. However, large offset and long record time (Table 1) are used for COCORP field surveys in order to probe deeper levels of the crust. To enhance both shallow and deep reflections recorded in such surveys, particularly highly attenuated deep reflections, extra care is needed in selecting appropriate processing steps and their parameters to attack the identified seismic problems.

The major seismic problem of the COCORP Michigan data appears to be persistent low-frequency noise. Obscured by this noise, the reflections on the original stacked sections are generally weak and lack continuity. This problem becomes more serious on the lower part of the sections. Virtually no reflections are visible below about 5.0 s (Figure 3). The noise can be clearly identified on field records such as that shown in Figure 4. This record is dominated by both coherent (e.g., A in Figure 4) and relatively incoherent (e.g., B in Figure 4) low-frequency noise. The coherent noise consists of successive parallel events with an apparent velocity of about 3.2 km/s. High-frequency noise is also evident on some traces (e.g., C in Figure 4), but its effect on the stacked data is minor.

In order to identify the frequency content of the noise and thus design appropriate processing steps to remove its effect, frequency analysis and filtering with different passbands were conducted. As a typical example, the amplitude spectrum of the upper 8 s of data from trace 12 in Figure 4 shows that the energy is concentrated within a narrow band about 10 Hz (Figure 5). Similar features are also shown by the spectra from other time windows. With high-pass filtering (20-32 Hz band pass), reflections are much clearer (e.g., between 2.0 and 4.0 s, Figure 6). In contrast, after low-pass filtering (8-15 Hz band pass), no reflections are visible on the filtered record (Figure 7). This suggests that the low-frequency part of the spectrum is dominated largely by noise, whereas the weaker high-frequency components contain more useful signal.

This persistent low-frequency noise is probably due to a near-surface low-velocity layer (SLL) as the Michigan Basin is covered by unconsolidated glacial drift with a maximum thickness of about 240 m [Landes, 1970]. As part of the processing, the shallow velocity structures were estimated from the first refracted arrivals of selected records using a τ-p inversion technique [Kennett, 1976]. The results show that the thickness of the SLL in the survey area is about 130 m. In general, the velocities increase rapidly from about 2.0 km/s near the surface to about 3.2 km/s at the base of the SLL. Below the base of the SLL, the velocities increase much more slowly and reach about 5.4 km/s at a depth of 1.2 km. Lateral velocity variations in the SLL are largest near the surface and diminish with depth. The average velocity at the base of the SLL is about equal to the apparent velocity of the coherent noise, indicating that these noise trains probably represent multiply reflected refractions in the SLL [Sheriff and Geldart, 1983]. A large portion of energy in an individual record, however, appears as less coherent noise, as indicated by the frequency-wave number (F-K) spectrum of the data (Figure 8). Figure 8 shows that the energy is concentrated between 8 and 16 Hz, but the majority of contours appears to be randomly distributed. This spatially "random" noise is suspected to be composed of reverberations and scattered waves trapped in the inhomogeneous SLL.

The lateral changes of velocity and thickness of the SLL will also causestatics variations [McClintock, 1975]. While long-wavelength statics variations introduce spurious structures, short-wavelength variations deteriorate data resolution and even destroy event continuity.

To attack these seismic problems, particularly the low-frequency noise, the processing sequence listed in Table 2 was developed from data analyses. The processing steps in this sequence, which were particularly effective in improving the seismic sections, are reviewed below. We include this detailed review here also because the published accounts of COCORP processing are rare and this review serves as a case study of current COCORP technique.

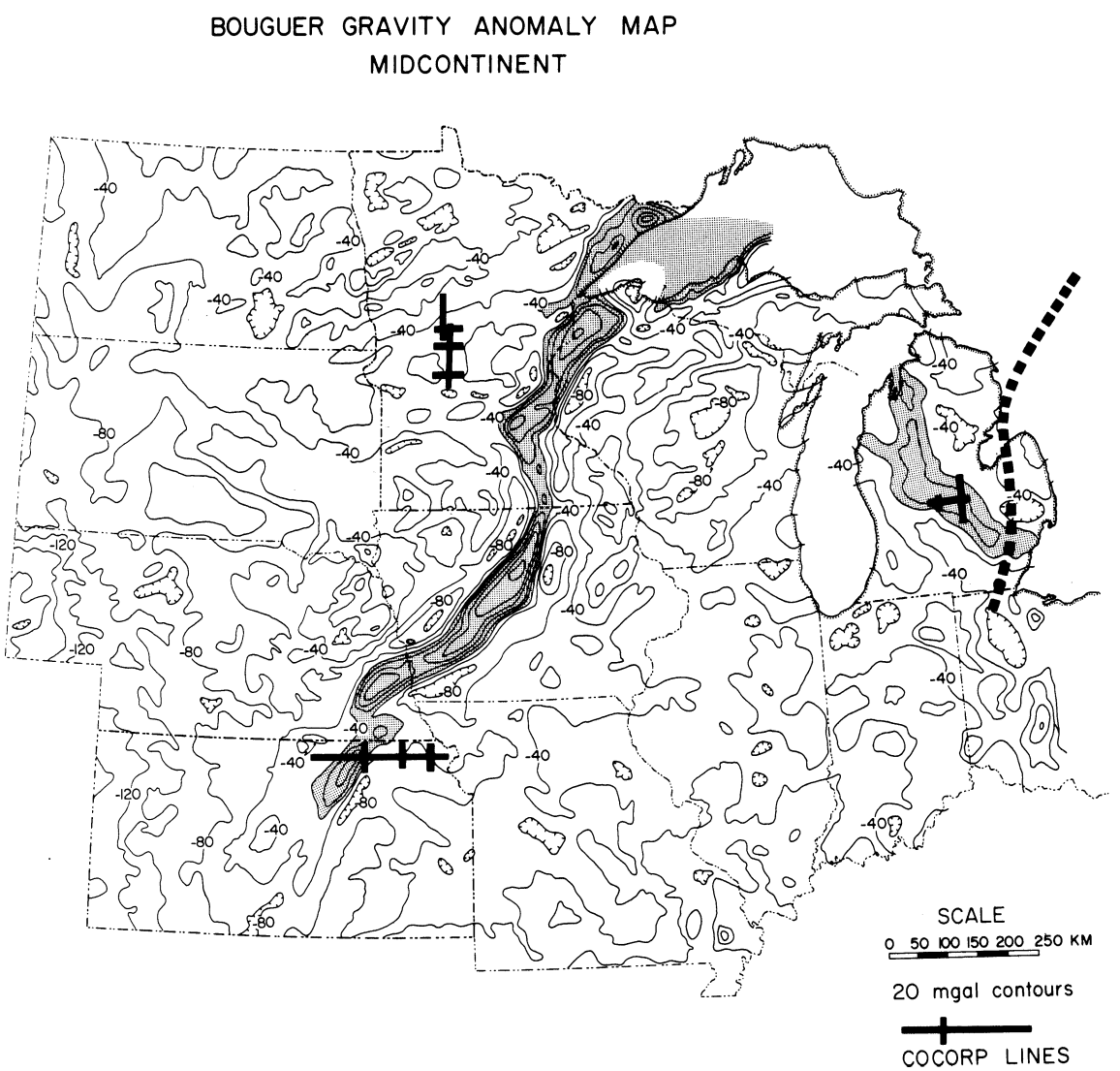

Fig. 2. Midcontinent Geophysical Anomaly and mid-Michigan gravity high (stippled [from Woollard and Joesting, 1964]), and locations of nearby COCORP surveys (heavy lines) (modified from Serpa et al. [1984]). Dashed line indicates the approximate position of the Grenville front [after Hall, 1978].

Reprocessing

As shown in Figure 3, the low-frequency noise which dominates the field records was not very well suppressed by common depth point (CDP) stacking in the original processing (Table 2). Nor does frequency and velocity filtering applied to the stacked sections improve the data quality significantly (compare Figures 9a, 9b and 9c). Thus attention was turned to removing the noise before stacking.

Computer-simulated trace mixing, or wave number filtering, was performed on the field records but was ineffective. Since the noise is in a narrow band close to the low-frequency end of the signal spectrum, high-pass filtering such as that used in Figure 5 was tried and found relatively effective in removing the low-frequency noise. However, such simple frequency filtering may also be eliminating desirable signals which lie outside the passband. For example, the low frequencies may well be important in defining deep structures. It was found that a more desirable approach for attenuating the low-frequency noise was deconvolution and velocity filtering before stack.

Deconvolution

Deconvolution, a widely used procedure in reflection seismology, is usually thought of as a means for increasing resolution by compressing seismic wavelets and for multiple suppression. In our data it also serves to reduce both random noise and the noise associated with the low-frequency spectral burst. This can be seen by considering the basic convolution model [e.g., Sheriff and Geldart, 1983]

$$x(t) = r(t) * w(t) + n(t) \qquad (1)$$

where $x(t)$ is a seismic trace, $r(t)$ reflectivity function, $w(t)$ equivalent wavelet, and $n(t)$ the noise. Deconvolution involves finding and apply-

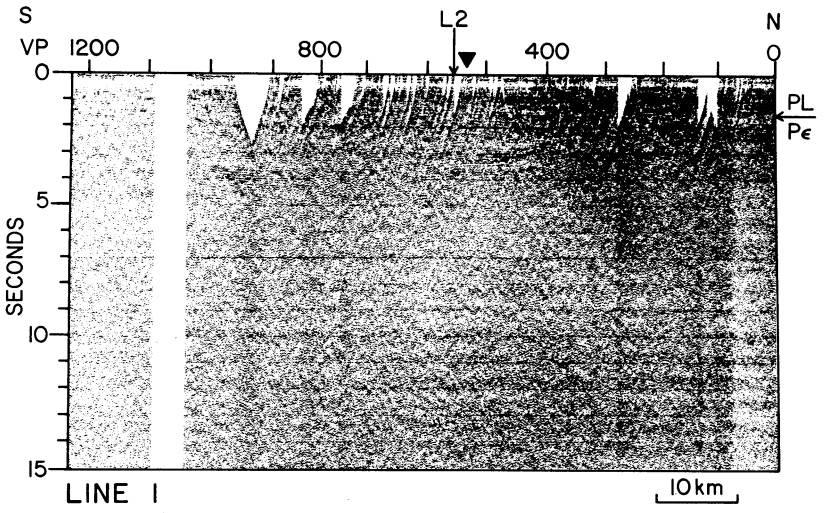

Fig. 3a. Original stacked section of Michigan line 1. Triangles indicate the projections of the deep well. No vertical exaggeration at a velocity of 6.0 km/s.

ing a filter d(t) which best compresses w(t) into a more impulsive wavelet i(t):

$$X(t) = x(t)*d(t) = r(t)*w(t)*d(t) + n(t)*d(t)$$
$$= r(t)*i(t) + n(t)*d(t) \qquad (2)$$

Thus the reflectivity function r(t) is better resolved on the deconvolved trace X(t) because of shorter duration of i(t). On the other hand, the convolution of d(t) with n(t) in (2) also tends to average out the random components in n(t) and attenuates the noise at frequencies where the wavelet w(t) is strong.

In this study, predictive deconvolution [Robinson and Treitel, 1980] was used with its operator length and predictive distance chosen from autocorrelations of the field records. Trace amplitudes were balanced before deconvolution, and four time windows per trace were employed in order to reduce various time-varying effects on deconvolution effectiveness. Figure 10 shows the record after deconvolution. It can be seen that reflections are now more identifiable than those on Figure 4. That deconvolution has reduced the contribution of random noise is apparent from comparing Figure 11 with Figure 8, the former dominated by coherent energy (e.g., A) and energy with high apparent velocities. Figure 12 shows that the spectrum of the data is now balanced due to the suppression of the low-frequency components. It is fortunate that the primary noise in the data is limited to low frequencies which the deconvolution filter d(t) was designed to attenuate. Had the weak high-frequency components of the data consisted largely of noise, deconvolution would have degraded the data by bursting the high-frequency noise [Lindseth, 1978].

Velocity Filtering

In addition to the prestack deconvolution, we found that velocity (F-K) filtering was also an effective tool for suppressing the noise in our data. F-K filtering distinguishes signal from noise based on their different apparent velocities. Their identification and separation are typically carried out in the F-K domain. The F-K filter applied to our data enhances the signal-to-noise ratio (S/N) by rejecting the noise energy within a specified apparent velocity range. This reject process is more attractive than either frequency or wave number filtering alone for recovering the extremely weak deep reflections: frequency filtering will eliminate the low-frequency components of the signal, while wave number filtering may reduce desirable high-frequency components. F-K filtering, on the other hand, can eliminate the noise without resorting to wholesale removal of certain frequencies. To preserve the frequency content of the signal, the frequency passband of the F-K filter used in this study was set to be equal to the bandwidth of the signal (8-32 Hz, Table 1).

Figure 13 shows the F-K spectrum of the record in Figure 4 after deconvolution and F-K filter-

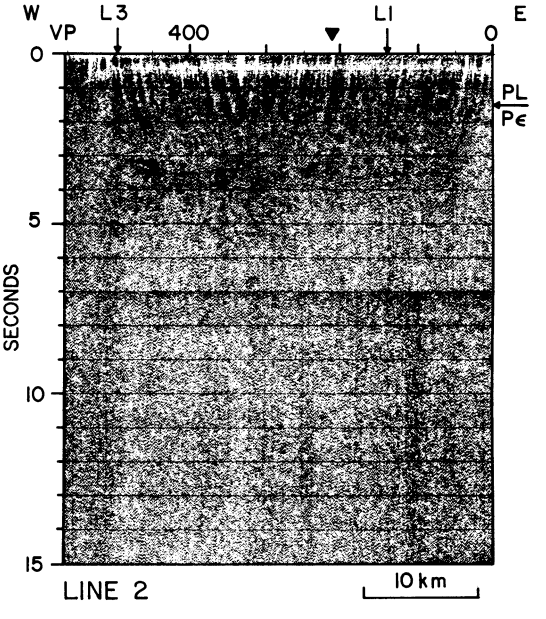

Fig. 3b. Original stacked section of Michigan line 2.

TABLE 1. Data Acquisition Parameters

Parameters	
Source	Vibroseis (TM Continental Oil Company)
	5 vibrator array
	16 sweeps/VP
	8-32 Hz upsweep
	30 s duration
	134-m (440 ft) spacing
Receiver	67-m (220 ft) station spacing
	96 channels off end
	near 268 m (880 ft) nominal offset
	far 6700 m (22000 ft) nominal offset
Recording	50-s recording time
	20-s correlated record length
	8 ms sample rate
	24 (nominal) fold
Record date	Aug. to Oct. 1978

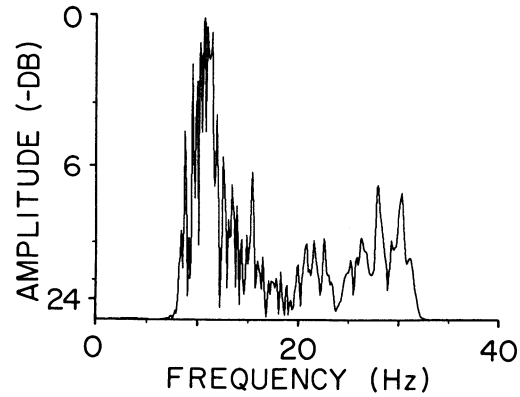

Fig. 5. Amplitude spectrum of trace 12 in Figure 4 (indicated in Figure 4 by triangle) after TAB.

ing. Comparison with Figure 11 indicates that this filter has removed both coherent and incoherent noise within the specified reject wedges on the F-K plane (Figure 13) yet has not significantly altered the frequency content of the data (compare Figures 12 and 14). Reflections are now much more prominent and continuous (Figure 15). Reflections as deep as 6.0 s can be more clearly traced.

Figure 16 shows the difference between a typical amplitude-balanced record and the same record after deconvolution and F-K filtering have been applied. Thus it represents the energy that was removed by this processing. Comparison with Figure 4 confirms that both coherent and incoherent noise has been attenuated. Note that multiply reflected refractions appear more clearly on Figure 16 (indicated by A), as do backward reflected refractions (indicated by B), which may be caused by irregularities near the base of the SLL [Sheriff and Geldart, 1983].

A danger in F-K filtering is spatial aliasing [March and Bailey, 1983]. In addition to causing possible aliasing of noise into the signal region, spatial aliasing also limits the reject boundaries in the F-K plane, particularly the lower boundary. If the dips of the boundaries of a reject wedge on the F-K plane are too small, the reject wedge may also be aliased back into the signal region and cut off the high-frequency components in the desired passband (L. Zheng and L.D. Brown, manuscript in preparation, 1986). Subsequently, a relatively small reject wedge, from 12 ms/trace (5.5 km/s) to 27 ms/trace (2.5 km/s) (Figure 13), was chosen based on results from F-K analyses and filtering tests to eliminate the dominant noise energy on the F-K plane

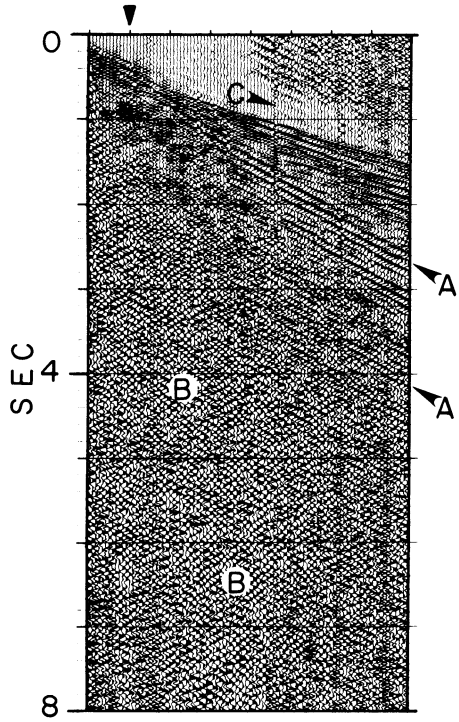

Fig. 4. A typical field record from line 2 (VP 13) after trace amplitude balancing (TAB). A and B indicate the coherent and incoherent noise, respectively.

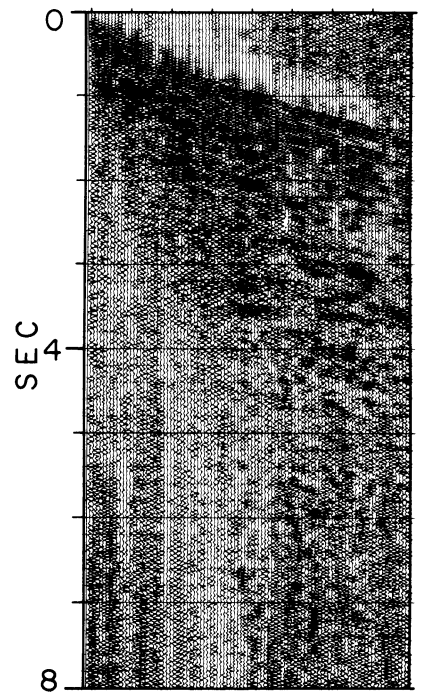

Fig. 6. The record shown in Figure 4 after TAB and 20-32 Hz band pass filtering.

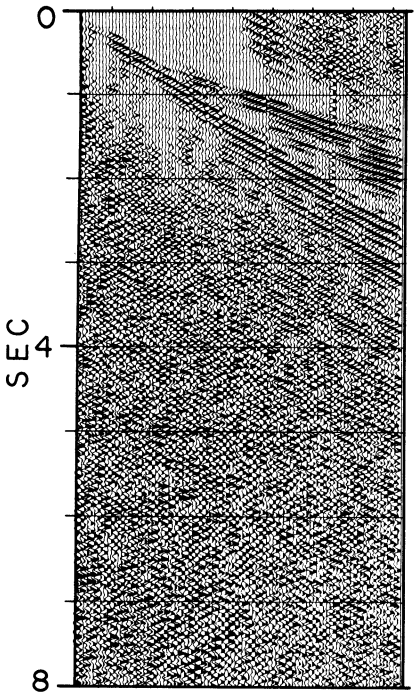

Fig. 7. The record shown in Figure 4 after TAB and 8-15 Hz band pass filtering.

(Figure 11), although a small amount of low-frequency noise was retained (Figure 13).

Apparent artifacts introduced by F-K filtering are small subhorizontal alignments (Figure 15). In general, these alignments are traceable for only a few traces and vary irregularly from record to record, suggesting that they are spurious effects introduced by F-K filtering. Some may be fortuitous coherences emphasized by the filtering, while others are probably caused by smearing of noise bursts by the filtering [March and Bailey, 1983; Christie et al., 1983]. These spurious alignments, together with the low-frequency noise remaining from the F-K filtering, will be further attenuated by CDP stacking because of their incoherent nature.

Stacking Velocity Estimation

The benefits of improving S/N from early deconvolution and F-K filtering cascade into subsequent processes. Inparticular, stacking velocities can be more clearly estimated from the improved data. Since these velocities are the critical parameters for the CDP stacking process, the signal enhancement effects of prestack deconvolution and F-K filtering are magnified.

Current approaches for determining stacking velocities are based on the hyperbolic approximation of reflection travel time curves, which theoretically is valid only when a medium is composed of horizontal, homogeneous layers and the ratio of offset to reflector depth is small. Both assumptions are often violated by COCORP data because of the long offset (up to 7-10 km) and complex deep structures involved in COCORP surveys. Nevertheless, the hyperbolic approximation is robust and works reasonably well for deep reflection data [Steiner, 1984]. However, such stacking velocities may lead to unacceptable errors if used to calculate interval velocities [Steiner, 1984; Liu et al., 1986].

Stacking velocities were carefully determined in this study by combining velocity semblance [Taner and Koehler, 1969], velocity scan, and constant velocity stacking [e.g., Dobrin, 1976] methods. Velocity semblance plots were generated at about every 40 stations. Relatively precise stacking velocities can be picked on a semblance plot because the semblance is calculated with small time and velocity increments (Figure 17). Very often, however, such semblance plots do not distinguish between legitimate reflections and spurious alignments of noise. Therefore velocity scans at larger increments were used to verify that the picked velocities correspond to credible reflections. The velocity scans used in this study produce both constant velocity stacks and displays of a normal-moveout-corrected CDP gather with a series of velocities for a selected CDP set. Velocities between analysis points were linearly interpolated. This interpolation, however, may not be adequate where lateral velocity variations are large. Thus constant velocity stacks of entire lines at several velocities were used to guard against overlooking rapid contrasts. Where such contrast was detected, velocity structure was refined by filling in with velocity semblance plots or velocity scans using relatively small time and velocity increments.

As pointed out previously, the velocity analysis was substantially aided by the prestack deconvolution and F-K filtering. Figure 17 shows velocity semblance plots for a CDP gather of line 2 near the deep well. The semblance plot from the earlier basic processing stream (Figure 17a and Table 2) is markedly inferior to that produced after the more elaborate processing used in this study (Figure 17b and Table 2). Semblance peaks are more scattered in Figure 17a, and velocities are virtually impossible to pick with confidence below about 3.6 s. In contrast, the semblance peaks from enhanced processing have higher values and are clearly defined, and optimum stacking velocities can be picked to about 6.2 s on the plot. Below that, semblance peaks become scattered and broadened, and stacking velocities were determined largely from velocity scans and constant velocity stacks. Figure 18 shows stacking velocities picked from

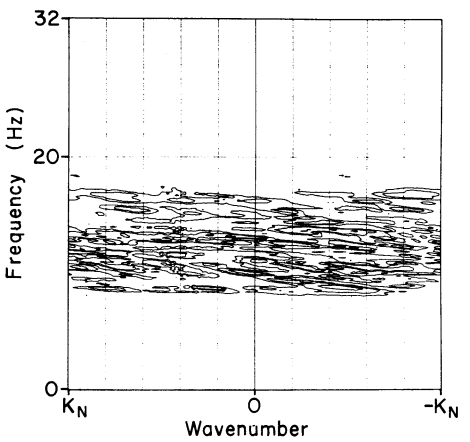

Fig. 8. F-K spectrum of the record shown in Figure 4, Nyquist wave number K_N = 0.0075/m.

TABLE 2. Data Processing Sequence (Following Demultiplex and Vibroseis Correlation)

Original Processing	Reprocessing*
1, Sort into common depth point (CDP) gather	1, Trace amplitude balancing (TAB)
2, Datum statics (elevation static correction)	2, Deconvolution
3, Velocity analysis (stacking velocity estimation)	3, Velocity filtering (reject)
4, Trace suppression (Mute)	4, Sort into CDP gather
5, Normal moveout correction	5, Datum statics (elevation static correction)
6, Automatic residual static correction (ARSC)	6, Velocity analyis (stacking velocity estimation)
7, 24-fold CDP stack	7, Trace suppression (Mute)
8, Deconvolution	8, Normal moveout correction
9, Filter	9, Automatic residual static correction (ARSC)
10, Automatic gain control (AGC)	10, 24-fold CDP stack
	11, Velocity filter (pie slice)

*Coherent filter has been applied to the sections shown in Figures 20a and 23.

Figure 17b and semblance plots computed at two other VPs near the deep well, as well as the corresponding velocity function from the original processing. Except for those corresponding to a reflection-poor zone (about 1.4-2.8 s), the velocities determined from the improved data are spatially consistent. In the shallow part the velocities from the reprocessing are higher than those used in the original processing and are more consistent with the results from an inversion technique discussed below.

Static Corrections

To minimize statics variations caused by the lateral velocity variations in the SLL, average velocities above a fixed datum were calculated every 50 stations from the shallow velocity structures estimated from the first refracted arrivals and used to compute elevation static corrections. Automatic residual static corrections (ARSC), derived from cross-correlation of traces in each CDP gather [Taner et al., 1974], were then used to reduce the residual short-wavelength statics variation. ARSC often improved the quality of reflections within the window chosen for analysis at the expense of data quality outside of the window, particularly when shallow windows were used. This inconsistency may indicate that the time shifts involved are not "static." Significant differences in the time shifts may occur between different arrivals of a single trace in COCORP data because of large offsets, long recording times, complex surface and subsurface geology, and irregular survey geometry. Calculations using a flat-layered velocity model derived in the next section indicate that the differences in time shifts caused by the SLL between shallow (0.6-1.4 s) and deep (3.0-6.0 s) events at a far trace are about 5-9 ms. These differences are comparable to ARSC computed from the data (most are about 10 ms) and may be increased by various factors such as lateral velocity variations and irregularities at the base of the SLL. To enhance deep reflections, the residual statics used in this study were computed from deep, long cross-correlation windows. Surface-consistent calculations seem to make no noticeable change in the cross-correlation shifts.

Figure 19 compares the stacked sections before and after ARSC from a 4.0-s correlation window starting at about 3.0 s have been applied. As expected, events below 3.0 s become smoother and more continuous (e.g., between 3.0 and 4.0 s). Outside the correlation window, some events (e.g., between 2.0 and 2.2 s) also appear to be more traceable after the corrections are applied. However, in general, the improvement of shallow events is marginal. Although some residual statics variations due to the SLL may remain uncorrected by the current application of ARSC, their magnitudes are generally small (less than 10 ms) compared to the breadth of source wavelets used in COCORP surveys (about 40 ms). Thus these residual statics variations may not significantly deteriorate the continuity of reflections in the data. Techniques for dynamic corrections of near-surface low-velocity layers are being developed [e.g., Kin and Jacewitz, 1984] which could prove useful for data of this type.

Figure 20 shows the reprocessed stacked sections of all three Michigan lines. Comparison between Figures 20 and 3 clearly demonstrates that the reprocessing has greatly improved the data quality by effectively eliminating the low-frequency noise and increasing resolution. Reflections are much more prominent and continuous on the reprocessed sections. Previously reported reflection patterns, particularly the bimodal appearance of the Keweenawan strata (i.e., a layered, highly reflective lower unit underlying a less reflective successor sequence), are now much more clearly defined and extended over a larger area. Furthermore, reprocessing also reveals new structural and stratigraphic details of the Keweenawan rift, and important reflections below 5 s that were entirely buried by noise on the original sections (e.g., E, F, and G in Figure 20a). These improved sections, along with the results from the following velocity and gravity modeling, provide a basis for a more

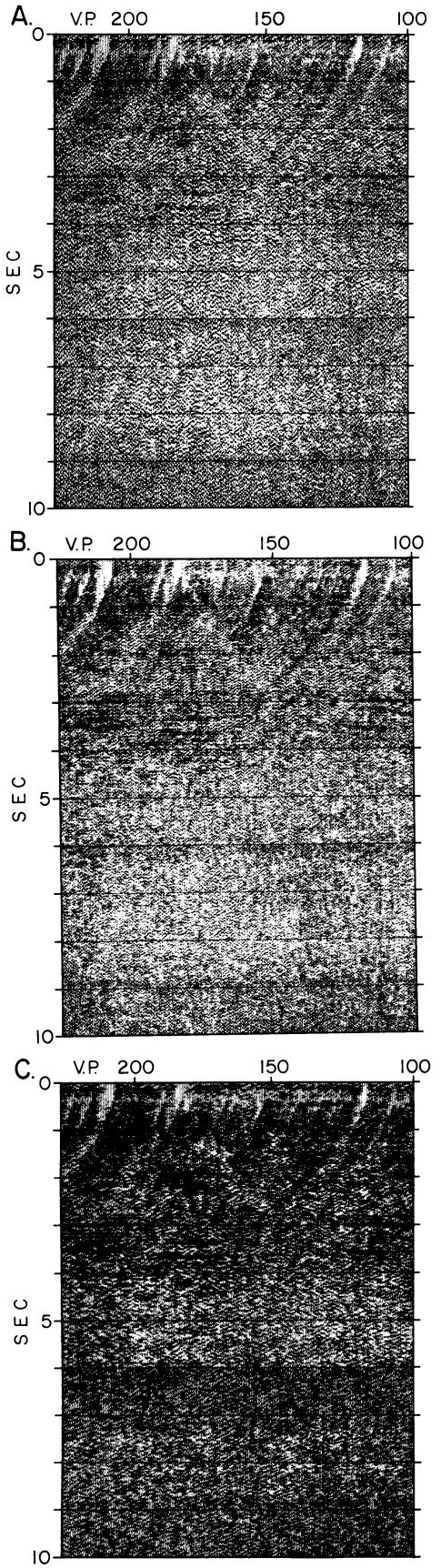

Fig. 9. Enlargements of the stacked section from line 2 between VPs 100 and 225: (a) original, (b) after poststack frequency filtering with 20-32 passband, (c) after poststack velocity (pie slice) filtering.

complete interpretation of deep structures beneath the Michigan Basin.

Velocity Measurement

A complementary goal in data processing is to deduce interval velocities from reflection data to aid interpretation. A common approach is to treat stacking velocities as rms velocities and compute interval velocities from these stacking velocities by the Dix equation [Dix, 1955]. This approach has been used in this study to estimate the interval velocities near the deep well (Table 3). The rms velocities used in the Dix equation were taken from the least squares fit shown in Figure 18, and the time intervals were determined based on the seismic units identified on the stacked sections (discussed later in detail). As pointed out previously, however, this approach may result in unacceptable errors in interval velocities for deep reflection data [Steiner, 1984; Liu et al., 1986]. As a comparison, a least-squares inversion techinque [Liu et al., 1986; Zhu and Brown, 1986] was used to calculate the velocities from reflection travel times. Two field records from line 2 near the deep well were selected for this calculation, and one of them is shown in Figure 21. Reflections were visually picked (Figure 21) and digitized. These travel time data were then inverted to yield the estimates of velocities and depths in Table 3. The usefulness of this technique depends on the ability to identify and trace individual reflections on a record. It is obviously sensitive to picking and correlation errors, particularly for deep reflections with small moveout [Zhu and Brown, 1986]. In this study, reflections R1 to R4 can be accurately picked. Reflection R5, however, is less certain. Nevertheless, reflection segments along R5 can be visually correlated and travel time picks for this reflection were guided by a smooth curve connecting the correlatable reflection segments. This correlation is strongly supported by the nearby semblance plots where the stacking velocities for R5 are well defined by strong semblance peaks near 6.2 s (Figures 17b and 18).

The resulting interval velocities and depths from these two different approaches agree reasonably well for some intervals and not so well for others. Larger interval velocities below layer B derived from the stacking velocities (Table 3) may be due at least in part to the known bias between stacking and rms velocities, which leads to erroneously high interval velocities [Al-Chalabi, 1974].

The high velocity of layer B estimated by the least squares method is consistent with that estimated from shallow refractions by τ-p inversion and also seems compatible with the lithologies encountered in the deep well (Figure 22), which include a large fraction of the Paleozoic limestones, dolomites, and evaporites [Landes, 1970; Hinze et al., 1978]. The underlying lower velocities of strata between 3.7 and 7.5 km are also consistent with Upper Keweenawan clastics found in the deep well.

Results and Interpretation

In many respects, the upper 5.0 s of the reprocessed sections confirms the basic features reported by Brown et al. [1982]. However, as

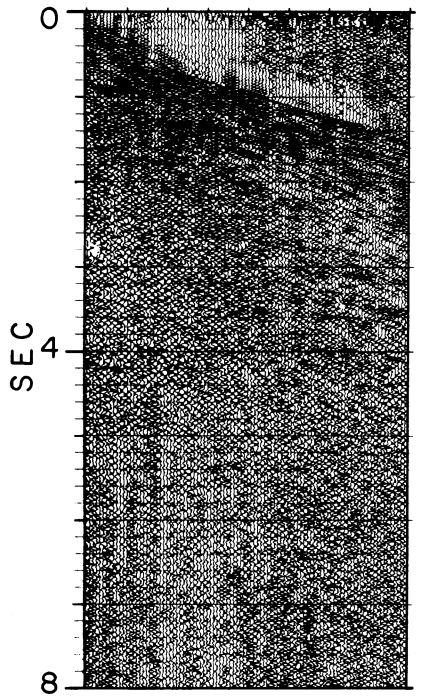

Fig. 10. The record shown in Figure 4 after TAB and deconvolution.

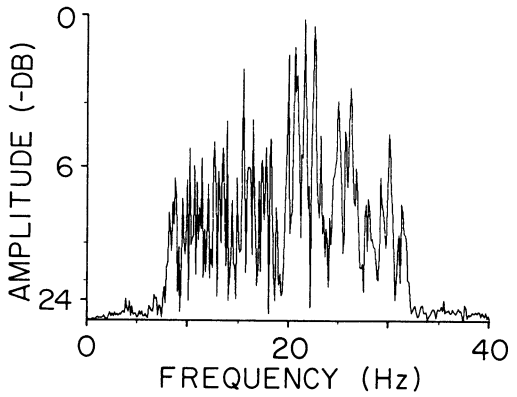

Fig. 12. Amplitude spectrum of trace 12 from Figure 10.

pointed out earlier, the three previously reported reflection units with different seismic characters are much better imaged by the reprocessing, and important structural and stratigraphic details can be seen for the first time. As a result, a more complete stratigraphic and structural interpretation of these units is now possible. Below 5.0 s, the reprocessed data reveal previously unrecognized deep reflectors which provide important new information on the deep structures beneath the Keweenawan strata.

Reprocessed sections clearly show that the flat-lying reflections of the upper 1.4 s or so are continuous across the survey area with little structural disruption and dip slightly toward the center of the basin (Figures 20 and 23). While obscured by the noise in the original sections, the base of this reflection unit is clearly marked in Figures 20a and 20b by the change in seismic character at about 1.4 s. The calculated thickness of this unit near the deep well (about 3.7 km, Figure 22) matches the thickness of Phanerozoic rocks from the well, which penetrated about 3.7 km of Phanerozoic section and 1.6 km of underlying Precambrian rocks [Sleep and Sloss, 1978]. Clearly, the upper unit corresponds to the nearly undeformed, slightly dipping Paleozoic strata of the Michigan Basin proper and its underlying Cambro-Ordovician sequence [Brown et al., 1982].

The less reflective character of the underlying zone from 1.4 to about 3.0 s is much more evident on the reprocessed sections (compare, e.g., Figures 20b and 3b). Based on this seismic character and the red bed sequence encountered near the bottom of the deep well [Fowler and Kuenzi, 1978], it is reasonable to interpret this zone as the Upper Keweenawan clastic assemblage [Brown et al., 1982], an inference also consistent with the regional geology. In the Lake Superior region this assemblage consists primarily of massive sandstones and conglomerates which seem less likely to produce prominent reflections [Sangree and Widmier, 1977].

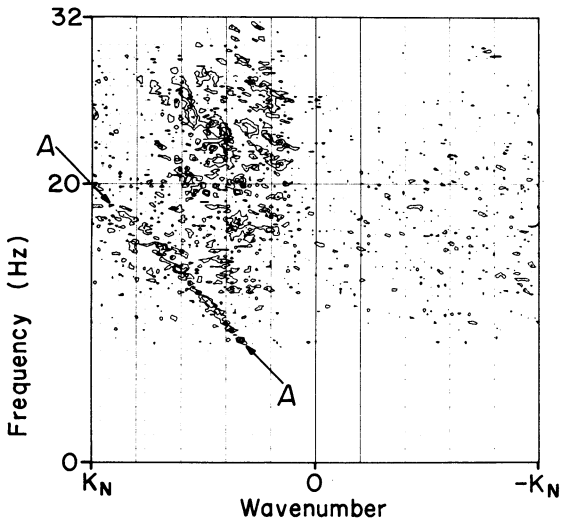

Fig. 11. F-K spectrum of the record shown in Figure 10. A indicates the prominent coherent noise shown in Figure 4.

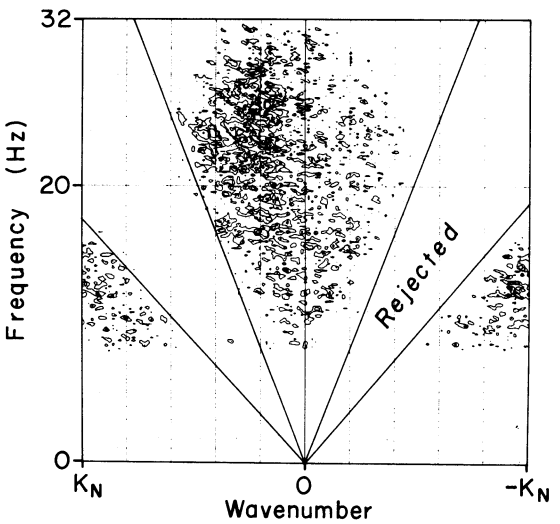

Fig. 13. F-K spectrum of the record shown in Figure 4 after TAB, deconvolution, and F-K filtering (reject).

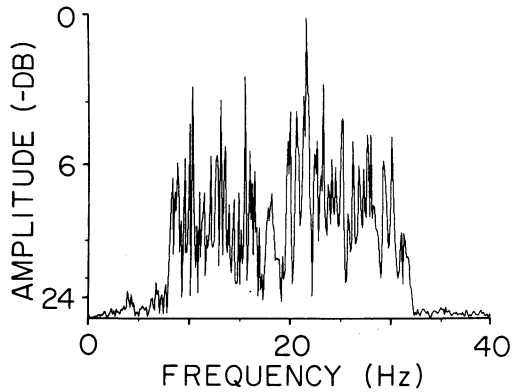

Fig. 14. Amplitude spectrum of trace 12 in Figure 4 after TAB, deconvolution, and F-K filtering.

The reprocessed data suggest for the first time two distinct subunits within this poorly reflecting zone (Figures 20a, 20b, and 23). The lower subunit consists of dipping reflections extending from about 2.1 to 3.0 s. This subunit is unconformably overlain by another subunit which consists of flat-lying reflections between 1.4 and 2.1 s, and which extends over a larger area on line 1 than the lower subunit. Although reflections in the upper subunit are relatively flat, most of them are unlikely to be multiples from the Paleozoic reflectors because (1) multiples should be highly suppressed in the reprocessing by deconvolution, F-K filtering, and CDP stacking with high stacking velocities (see, e.g., Figure 18), and (2) flat events sharply decrease in number below about 2.1 s and do not cross-cut deeper dipping events, and (3) their travel times apparently do not fit a simple multiple pattern.

The red bed sequence encountered by the deep well below the Cambrian consists of recurring beds of sandstones and mudstones and is similar to the sequence found by drilling on Beaver Island, 260 km to the north along the mid-Michigan gravity high [Fowler and Kuenzi, 1978]. The interpretation of the red bed sequence from the deep well is controversial, and various stratigraphic positions for this sequence have been suggested, including the Middle Keweenawan [Kalliokoski, 1982], the Upper Keweenawan Oronto group [Catacosinos, 1981; Ojakangas and Morey, 1982a], and Jacobsville sandstone [Hinze et al., 1978], and post-Jacobsville strata [Fowler and Kuenzi, 1978]. Here, we interpret the two subunits as the Jacobsville sandstone and the underlying Oronto group (or their equivalents) based on their unconformable contact and contrasting structural styles as exhibited on the seismic sections (e.g., Figures 20a and 20b). In the Lake Superior region, the unconformity between the subhorizontal Jacobsville sandstone and the relatively steeply dipping Oronto group has been indicated by various geologic observations [e.g., Craddock, 1972; Ojakangas and Morey, 1982a; Daniels, 1982] and is thought to represent an important transition between two different tectonodepositional environments [e.g., Craddock, 1972; Fowler and Kuenzi, 1978; Morey and Ojakangas, 1982]. The sharply tilted and folded Oronto group rocks accumulated in a narrow rift basin whereas the relatively flat-lying Jacobsville sandstone was deposited in a broad crustal downwarp perhaps caused by the foundering of the incipient rift [Fowler and Kuenzi, 1978]. Some of the relatively strong reflections within the unit may correspond to volcanic flows observed in the Oronto group sediments [White, 1966; Daniels, 1982] and to igneous horizons

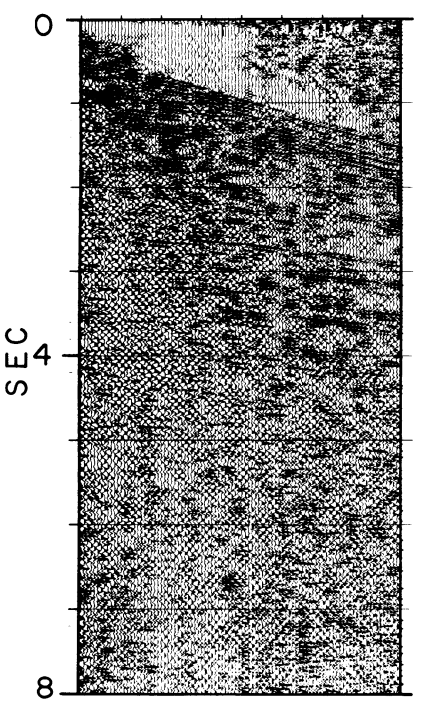

Fig. 15. The record shown in Figure 4 after TAB, deconvolution, and F-K filtering.

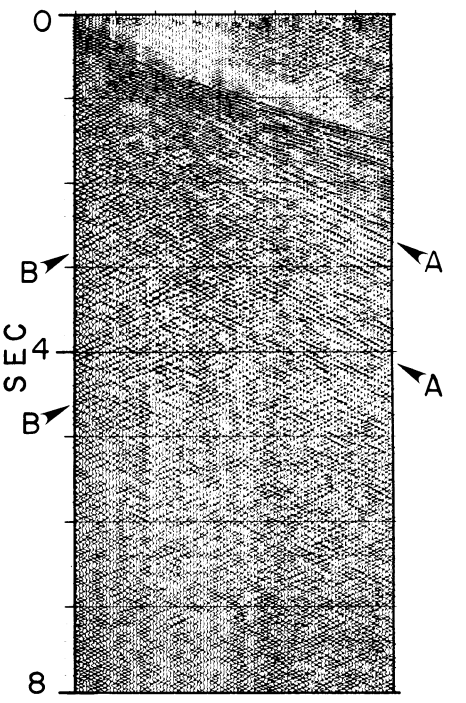

Fig. 16. Difference between records in Figures 4 and 15.

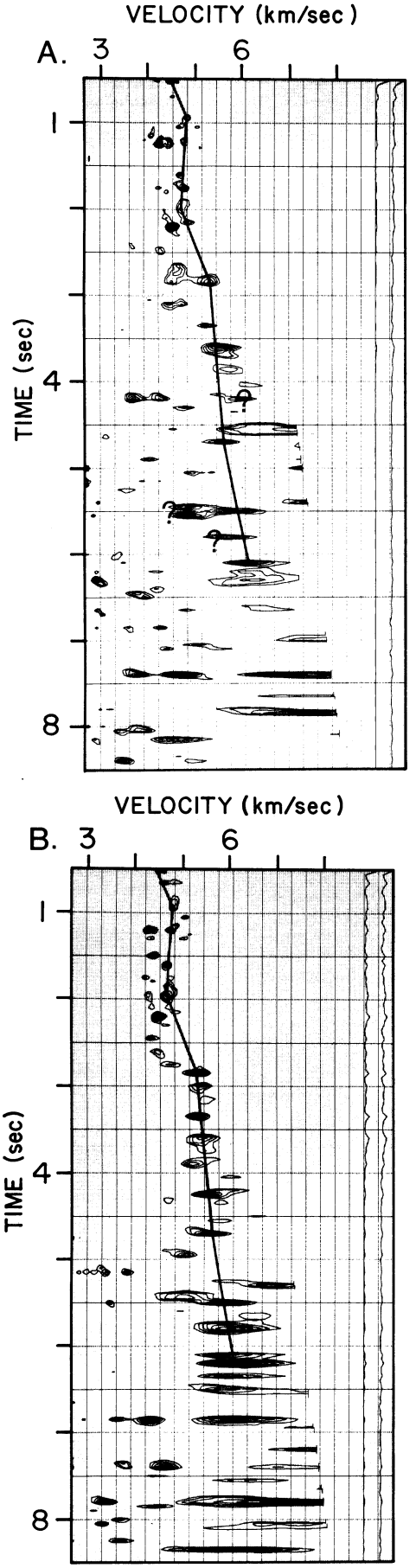

encountered by deep drilling below the Cambrian [McCallister et al., 1978].

The relatively prominent layered reflections from 3.0 to 5.0 s imaged on the original sections define a structural trough (Figure 3a) which coincides spatially with the mid-Michigan gravity high. On the basis of this correlation, overall seismic character, and regional geology, these deep reflections were interpreted as the Middle Keweenawan volcanic sequence [Brown et al., 1982], an interpretation also supported by the velocity profile in Figure 22. The Middle Keweenawan volcanic sequence of the Lake Superior region is composed of thick (more than 12 km) and extensive mafic volcanic flows (large flows have been traced laterally for up to 50-90 km) interbedded with subordinate clastics [Craddock, 1972; Green, 1982]. The velocities of such an interbedded sequence are expected to be higher than those of the overlying Upper Keweenawan clastic assemblage but lower than those of basalts [e.g., Dobrin, 1976]. The interbedding of lava flows and clastics also provides high impedance contrasts for generating the prominent reflections [Brown et al., 1982]. The early interpretation of this layered reflection unit is, however, limited by the poor quality of the original seismic sections. For example, the extent and geometry of the volcanic sequence are poorly defined in Figure 3. It is unclear whether the reflectors on the flanks of the trough are connected across the trough or disrupted by faulting. With the improved image brought about by the reprocessing, however, a more complete interpretation of this unit is now possible.

The layered reflection unit on line 1 (A, C, and D in Figures 20a and 23) extends about 100 VPs farther north on the reprocessed section than on the original and can clearly be traced to the south end of this line. Thus this unit defines an approximately 70-km-wide rift basin with relatively steep flanks. Its northern flank is represented by south dipping reflections between VPs 150 and 475, and its southern flank by north dipping events from VP 875 to the southern end of line 1. No evidence of a flank is seen on line 2, as expected, since line 2 is subparallel to the strike of the gravity high. Below 5.0 s the layered reflections become fewer and weaker, but prominent reflections continue to around 6.0 s beneath VPs 850 to 950 of line 1 as well as on parts of lines 2 and 3 (Figure 20). Thus the volcanic sequence may in some places extend to about 6.0 s, giving about 8 km for its maximum thickness. This inference is also supported by a gravity model described later which suggests high-density material below 14 km (5 s). The basin-like structure defined by this thick volcanic sequence is similar to the rift structure in the Lake Superior region [e.g., White, 1966] but differs from that revealed by the

Fig. 17. Velocity semblance plots of the CDP gather at VP 187 of line 2: (a) produced with the original processing sequence (Table 2), and (b) produced with the reprocessing sequence. Solid lines indicate the velocity function determined from Figure 17b. Question marks in Figure 17a indicate the scattered strong semblance peaks below about 3.6 s.

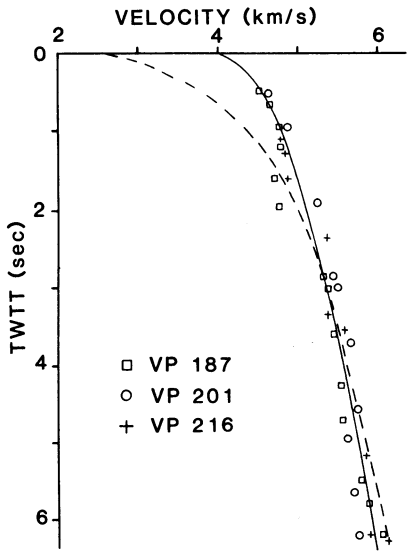

Fig. 18. Stacking velocities from three VPs (indicated by different symbols) of line 2 near the deep well and their least squares fit (solid line). TWTT refers to two-way travel time. Dashed line represents the corresponding velocity function used in the original processing.

COCORP Kansas survey on the southern end of the MGA where a relatively thin (maximum thickness about 4.5 km) volcanic sequence delineates a half graben [Serpa et al., 1984].

In addition to more clearly defining the geometry of the rift, the reprocessed data also revealed new structural and stratigraphic details which provide further information on the evolution of the rift. For example, the continuous and layered character and basinward thickening of the inferred volcanic sequence indicate that the rift basin was subsiding as it was being filled by episodic volcanic flows and interflow clastics [Craddock, 1972; Merk and Jirsa, 1982]. As shown on line 1 and line 2, the volcanic sequence is conformably overlain by the Oronto group sediments, suggesting that the rift basin continued to subside after the major volcanism had terminated [e.g., Craddock, 1972; Morey and Ojakangas, 1982].

North of about VP 450 on line 1 the reflections in sequence A become weaker and discontinuous, but some events can still be traced to about VP 250. These weak reflections are arched, ending against a set of south dipping events (C in Figures 20a and 23) which extend from VPs 150 to 350 and become weaker and less continuous but still traceable beyond VP 350. South of the data gap (from VPs 1015 to 1065), reflections in sequence A are weak. They also appear to be arched and terminate against a set of north dipping events (D in Figures 20a and 23) which may be correlated with C and form the deeper part of the volcanic sequence. Although reflections in sequence A are weaker and less continuous in the central part of the rift basin, they can clearly be traced across the basin on the reprocessed section of line 1 (Figure 20a). There is no evidence that the changes in seismic character toward the center of the basin are due to the variations in the surface geology and/or data acquisition conditions. These changes may reflect either the lack of clastics and/or variations in the interflow clastic components toward the center. The reflectors in sequence A are generally concordant except near the west end of line 2, where a triangular zone (B in Figure 20b) appears to separate the curved events above from nearly planar events below. Sequence A and the overlying inferred Oronto group are broadly bent, and a sharp flexure occurs near VP 460 on line 1.

The volcanic sequence and Oronto group shown on line 1 appear to have been rotated as a block,

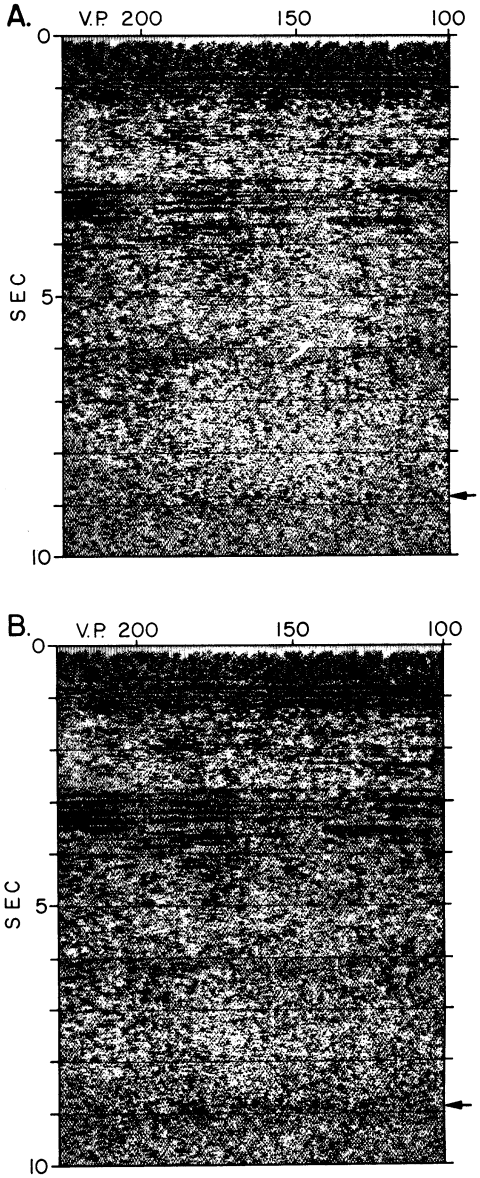

Fig. 19. Reprocessed stacked section of the same data as those shown in Figure 9: (a) without and (b) with automatic residual static corrections applied. Note that subhorizontal reflections near 9.0 s are now evident on the sections (indicated by the arrows).

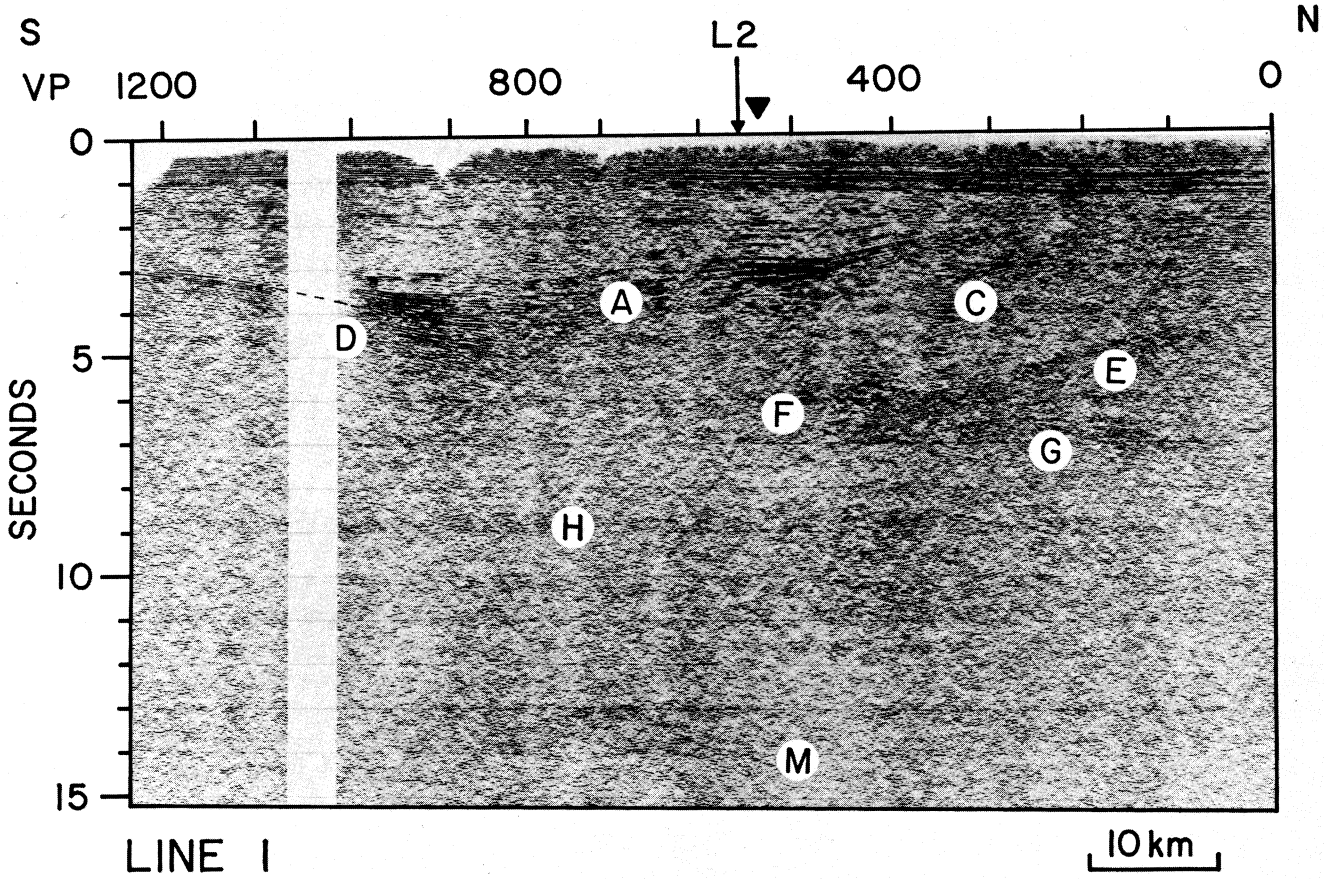

Fig. 20a. Reprocessed stacked section of Michigan line 1. Triangles indicate the projections of the deep well. No vertical exaggeration at a a velocity of 6.0 km/s.

making the south flank about 1.0 s (3 km) deeper than the north flank (Figures 20a and 23). At their north end these strata were apparently eroded and are unconformably overlain by the Jacobsville sandstone. There is no unequivocal evidence that the Jacobsville sandstone was also affected by the tilting, although scarcity of strong marker reflections may have prevented the recognition of such evidence.

One possible interpretation for this crustal tilting is that it was caused by normal faulting and/or crustal thinning. This would imply a post-Oronto extension. There seems to be no reported geologic evidence to substantiate such late Keweenawan extension. In contrast, the regional geology of the Keweenawan rift indicates a post-Oronto compressive episode [e.g., Craddock, 1972]. In the Lake Superior region the compressive event is characterized by folding and reverse faulting. While the formation of the folds in that area may be dated as post-Oronto but pre-Jacobsville, the major movements of reverse faults (e.g., Keweenawan fault) were perhaps completed by the end of Jacobsville time [Craddock, 1972]. Some authors [e.g., Hall. 1978; Watts, 1981] have suggested that the compressive phase was related to the Grenville Orogeny, based on the time overlap of Keweenawan and Grenville tectonism and the parallelism between the most prominent faults in the Lake Superior region and the Grenville front. Hinze et al. [1972] and Fowler and Kuenzi [1978], however, associated the late compressional features of the Keweenawan rift with mantle contraction resulting from thermal decay. A similar mechanism was also invoked by Hoffman [1973] to explain the late compressional features, including crustal downwarps, reverse faults, broad folds, and igneous activity, associated with the Athapuscow aulacogen of the northwestern Canadian shield. It is possible that the crustal tilting and some of the structures within the inferred volcanic sequence and Oronto group resulted from late Keweenawan compression. For example, the apparent truncation of A by C and D in Figures 20a and 23 may represent reverse faults rather than depositional lapout. Such reverse faults were also suggested by Hinze et al. [1975] and Fowler and Kuenzi [1978]. The arched reflections on both flanks could be drag folds. The triangular zone on line 2 (B in Figure 20b) might similarly represent blind thrusts rooted to the west of line 2. However, if these features are due to compression, they would seem to imply an approximately north-south compression, which is almost perpendicular to compression expected from the Grenville Orogeny (Figure 2). The data from the COCORP Kansas survey also contain a possible flanking reverse fault truncating the Middle Keweenawan volcanic sequence, although Serpa et

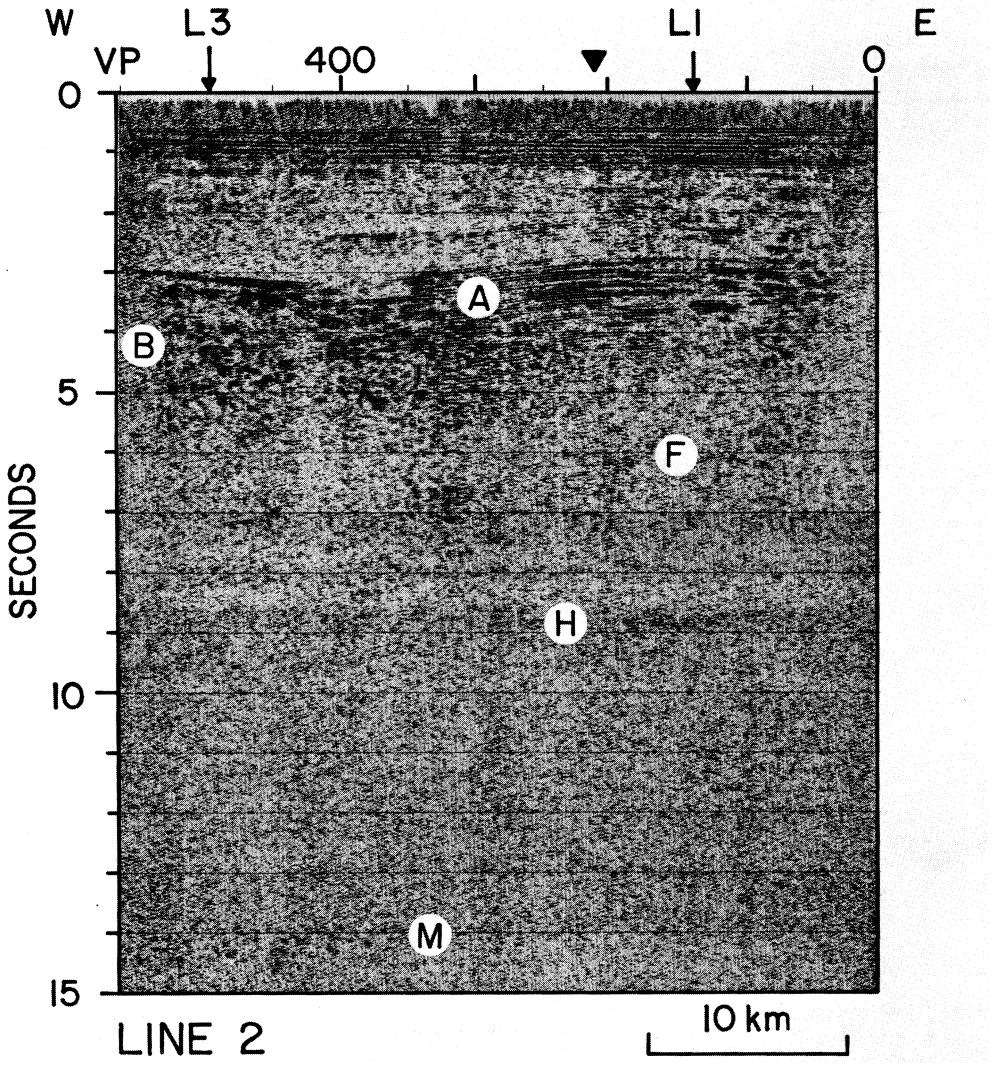

Fig. 20b. Reprocessed stacked section of Michigan line 2.

al. [1984] argued that other interpretations may be more plausible.

Perhaps the most impressive result of the reprocessing was to bring out deep reflections that were entirely buried by the noise on the original seismic sections. The most prominent of these is the dipping event E on the north half of line 1 (Figure 20a). Its apparent dip on line 1 is about 18°. The true three-dimensional dip is uncertain because it is difficult to identify this event on line 2.

F is a band of discontinuous but relatively prominent reflections that appear to be truncated by E near VP 400 on line 1 (Figure 20a). Between about VPs 350 and 500, these reflections are relatively flat, though beyond VP 500 they curve downward and become more and more difficult to trace. Events F on line 2 are more discontinuous with the most prominent segment near VP 320 (Figure 20b). Beneath E is another set of layered reflections (G in Figures 20a), which is also curved and appears to end against E.

Migration (Figure 23) and travel time modeling using the velocity profile in Figure 22 indicate that E, F, and G are not diffractions. There is also no geologic evidence suggesting that they are sideswipes from shallow structures. The extent, dip, and narrowness of E might indicate a fault. It may or may not be related to Keweenawan rifting or subsequent compression, and its proximity to the Precambrian basin raises the issue of whether it might be a reactivated fault. The identities of reflections F and G are unknown, though several plausible interpretations are possible, including Lower Keweenawan sedimentary rocks [e.g., Ojakangas and Morey, 1982b], a layered Keweenawan intrusion [e.g., Craddock, 1972; Weiblen, 1982], and a lower unit of the Keweenawan volcanic sequence. The observations in the Lake Superior region indicate that the volcanic sequence may be divided in two different units. Locally, the two units show slight discordance and may be separated by a clastic sequence [Hall, 1978].

Reflections from beneath E, F, and G are scarce. Yet on parts of line 1 and line 2 there are bands of weak subhorizontal reflection segments at about 9.0 s (H in Figures 20a and

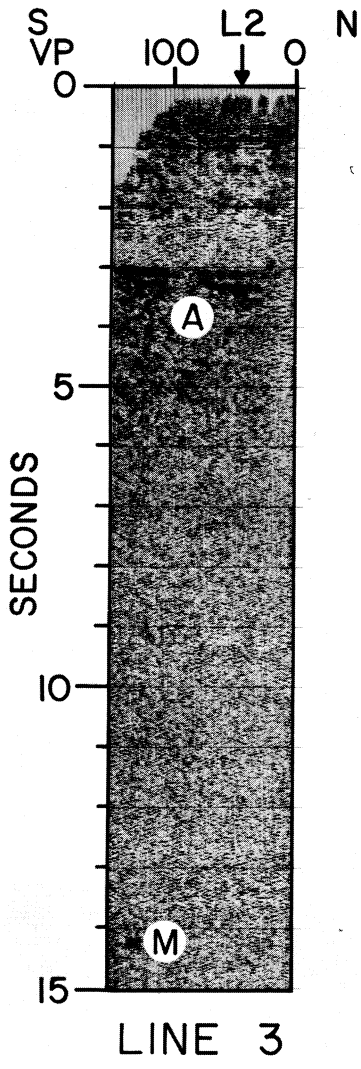

Fig. 20c. Reprocessed stacked section of Michigan line 3.

20b, indicated also in Figure 19 by arrows). The origin of these reflection bands is unclear. Although their depth (about 25 km) is comparable with that of the classical Conrad discontinuity, there is no report of such a discontinuity from deep refraction surveys in the nearby Lake Superior area [e.g., Smith et al., 1966], and the ubiquity of such a boundary has been called into question [Oliver, 1978].

A prominent reflection segment occurs near the south end of line 3 at 14.3 s (about 43 km; M in Figure 20c). Weak short reflection segments are also identifiable at about 14.3 s near the west end of line 2 and at about 14.0 s on parts of line 1 (M in Figures 20a and 20b). Below about 14.0 s coherent reflection segments on lines 1 and 2 are noticeably fewer. This loss of reflections, if not an artifact, may suggest that the material below 14.0 s is relatively homogeneous. Compilation maps of crustal thickness in the Lake Lake Superior region by Hall [1982] indicate that while the normal crustal thickness in that region is about 40 km, the depth of Moho in some areas near the axis of the Keweenawan rift may range from 45 km to perhaps more than 50 km. Therefore the reflections near 14.3 s, tenuous though they are, are good candidates for Moho reflections.

Many reseachers have attempted to model the gravity field associated with the Keweenawan rift [e.g., Hinze et al., 1975]. Here we use the seismic data as a guide for a fresh attempt. The crustal model used in two-dimensional gravity modeling is shown in Figure 24, along with its computed gravity effects and the observed Bouguer gravity anomaly along line 1 [from Hinze et al., 1971]. This model is constructed based on the subsurface interpretation summarized in Figure 23, and the velocity profile shown in Figure 22. Obviously, the two-dimensional assumption must be suspect since the lines are near a bend in the trend of the gravity field, so that line 1 is not strictly perpendicular to structure. Nevertheless, as a first-order approximation, two-dimensional modeling seems appropriate. An

TABLE 3. Estimated Velocities and Depths and the Interpreted Stratigraphy Near the Deep Well

	Dix Equation		Least Squares Inversion		Interpreted Stratigraphy
Layer	V	D	V	D	
A	2.3	0.13	2.3	0.13	SLL (mainly glacial drift)
B	5.3	3.5	5.6	3.7	Phanerozoic
C	5.6	5.4	5.5	5.6	Upper Keweenawan
D	5.8	7.5	5.3	7.5	clastics
E	6.2	11.3	5.7	11.0	Middle Keweenawan
F	6.6	18.0	5.9	17.1	volcanic sequence

V, layer velocity (km/s). D, depth to the lower interface of a layer (km). Note that V and D for layer A are estimated from first refractions.

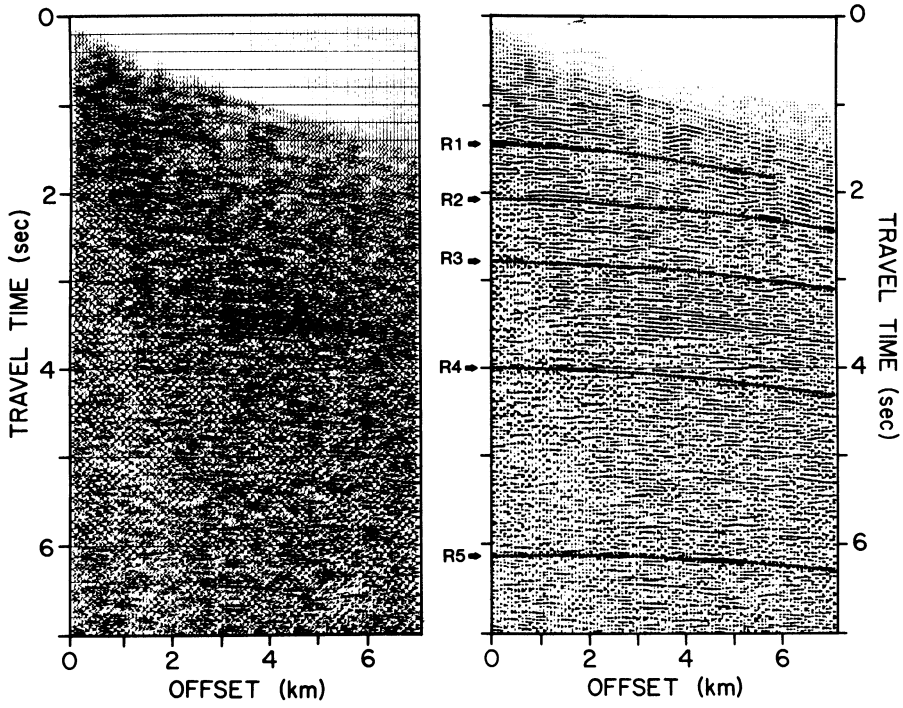

Fig. 21. The field record at VP 199 of line 2 and travel time picks (indicated by R_n) used for the velocity calculation.

average density of 2.61 g/cm^3 for the Phanerozoic column was adopted from the measurements in the deep well [Hinze et al., 1978]. The density of 2.65 g/cm^3 for the Oronto group, 2.95 g/cm^3 for the volcanic sequence, and 2.70 g/cm^3 for country rocks of the upper crust in the model are similar to the values used by many investigators in their gravity studies of the Midcontinent rift system [e.g., Hinze et al., 1982]. The density for the Jacobsville sandstone is less certain. Possible values include those close to 2.40 g/cm^3, as used by many investigators, or two rather high-density values determined from deep well by sample cuttings, 2.72 g/cm^3, and by the borehole gravimeter, 2.77 g/cm^3 [Hinze et al., 1978]. Since the higher borehole gravimetric density may be due to the effect of mafic igneous rocks within the Jacobsville sandstone surrounding the hole [Hinze et al., 1978], values of 2.40 and 2.72 were chosen for the density of the Jacobsville sandstone in separate gravity calculations. As it turns out, the gravity anomaly is relatively insensitive to the density of the Jacobsville sandstone since it is relatively flat.

The gravity profile calculated from the crustal model agrees well with the observations (Figure 24). Although this model is by no means unique, it is well constrained by the seismic data. The model would seem to suggest that a high-density body exists below about 14 km (5 s) beneath the north flank of the rift basin, indicating that F may represent mafic rocks. On the other hand, the model clearly demonstrates that gravity anomaly in the COCORP survey area does not require a high-density body in the lower crust or a lower-density body beneath the Moho as suggested for other areas along the Keweenawan rift system [e.g., Chase and Gilmer, 1973; Hinze et al., 1982].

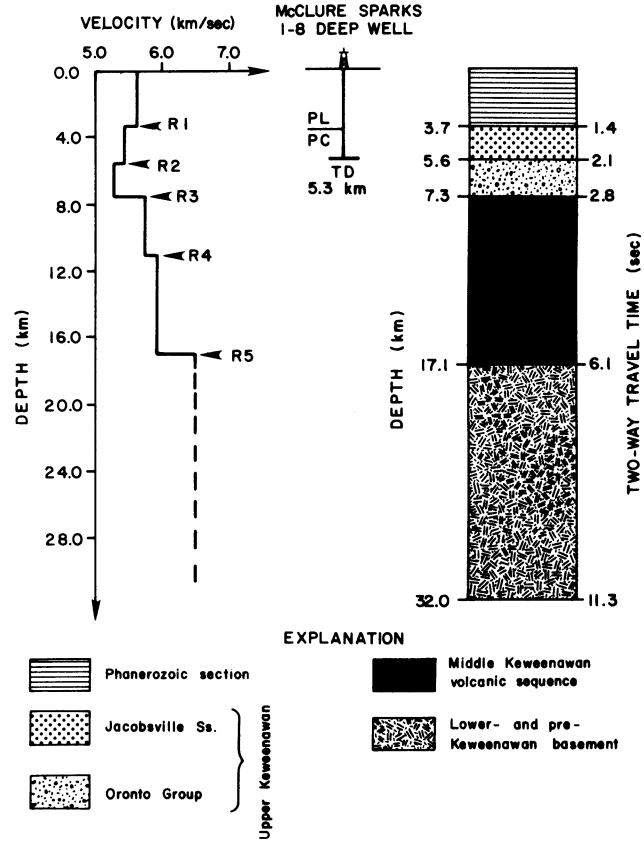

Fig. 22. Velocity profile estimated by the least-squares method (Table 3) and interpretive stratigraphic section near the deep well. Dashed line indicates the velocity (6.5 km/s) used for depth conversion below 6.1 s.

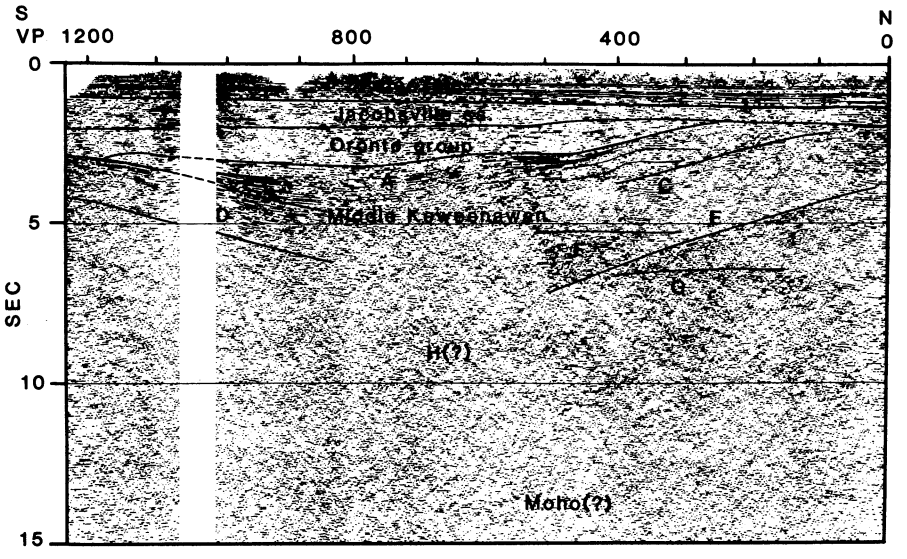

Fig. 23. Interpreted migrated section of line 1.

In spite of the improvement brought about by the reprocessing, there is still little unequivocal evidence on the seismic sections which enables us to decipher the cause of the Paleozoic subsidence of the Michigan Basin. If the weak midcrustal and "Moho" reflections are valid, their relative flatness could be significant to this problem. However, further tracing of the sub-Paleozoic reflectors, especially the Moho, toward the center of the basin is needed to provide information on this matter.

Summary and Conclusions

Deep reflection data represent an important new reservoir of geological information. That information is unlikely to ever be fully extracted during initial analyses, if for no other reason than the fact that our understanding of crustal geology is continually evolving. The reprocessing reported here, and by other investigators, is thus a natural component of any deep seismic profiling effort.

The quality of COCORP data from the Michigan Basin is severely degraded by low-frequency noise. This noise is identified as multiply reflected refractions, reverberations, and scattered waves trapped in a near-surface low-velocity layer and was not adequately suppressed by the basic processing sequence originally used. In this study, prestack F-K filtering and deconvolution were used and found to be highly effective in eliminating the noise and increasing resolution. With the substantially improved field records, subsequent key processing steps such as velocity analysis, automatic residual static correction, and CDP stacking become more effective. As a result, both shallow and deep reflections are greatly enhanced on the reprocessed sections. These improved sections, when coupled with regional geology and the results from velocity and gravity modeling also carried out in this study, yield significant new insight into the subsurface geology of the Michigan Basin.

As summarized in the interpreted section of line 1 in Figure 23, the reprocessed data confirm and much more clearly define the following:

1. The upper 1.4 s (3.7 km) or so of shallow flat-lying reflections represents virtually undeformed Paleozoic strata of the Michigan Basin proper and its underlying Cambro-Ordovician sequence.

2. The reflection-poor zone beneath the Paleozoic probably corresponds to about 4 km of the Upper Keweenawan clastic assemblage.

3. Reflections between about 3.0 and 6.0 s are highly reflective and layered, probably corresponding to up to 8 km of the Middle Keweenawan volcanic sequence which delineates an approximately 70-km-wide rift basin.

In addition, the reprocessed sections show for the first time the following:

4. The upper Keweenawan section is separated by an unconformity into two units with contrasting structural styles. These units probably correspond to the Oronto group and the overlying Jacobsville sandstone (or their equivalents). The unconformity between the two units represents

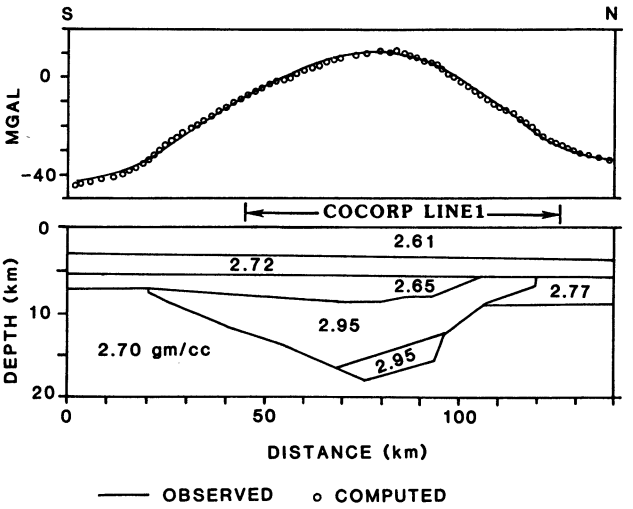

Fig. 24. Bouguer gravity model along line 1.

an important transition between two different tectonodepositional environments. While the Oronto group accumulated in a narrow rift basin, the Jacobsville sandstone was deposited in a broad crustal downwarp.

5. Newly imaged stratigraphic and structural features within the volcanic sequence and Oronto group provide further information on the evolution of the Keweenawan rift. For example, the continuous and layered character and basinward thickening of the volcanic sequence indicate that the rift basin was subsiding as it was being filled by episodic volcanic flows and interflow clastics. This subsidence continued after major volcanism was terminated as evidenced by conformable contact between the volcanic sequence and the overlying Oronto group. The post-Oronto crustal tilting and some structures seen in the volcanic sequence and Oronto group, on the other hand, suggest a possible late Keweenawan compression.

6. A south dipping event exists beneath the inferred volcanic sequence that may represent a major crustal fault, cutting two deep layered reflection bands.

7. Weak, deep reflection segments may exist near 9.0 s (25 km) and 14.3 sec (43 km). If these weak events are valid, the latter may be from the Moho.

Acknowledgements. We thank J. E. Oliver and A. Gibbs for critically reading the manuscript. Many of the ideas in this paper benefitted from discussions and presentations of many individuals within the COCORP project, particularly C. Caruso, L. Zheng, and J. Huang. Figure 16 in the paper was provided by G. Johnson. The τ-p inversion program used was implemented at Cornell by P. McGuire. The field data were collected by crew 6834 of Petty-Ray Exploration Service of Geosource, Inc. The data were reprocessed on COCORP's MEGASEIS (TM Seiscom Delta) system. This work was supported by National Science Foundation grants EAR 82-12445 and EAR 83-13569. Institute for the Study of the Continents (INSTOC) contribution 15.

References

Al-Chalabi, M., An analysis of stacking, RMS, average, and interval velocities over a horizontally layered ground, Geophys. Prospect., 22, 458-475, 1974.

Brown, L., L. Jensen, J. Oliver, S. Kaufman, and D. Steiner, Rift structure beneath the Michigan Basin from COCORP profiling, Geology, 10, 645-649, 1982.

Catacosinos, P. A., Cambrian lithostratigraphy of the Michigan Basin, Am. Assoc. Pet. Geol. Bull., 57, 2404-2418, 1973.

Catacosinos, P. A., Origin and stratigraphic assessment of pre-Mt. Simon clastics (Precambrian) of Michigan Basin, Am. Assoc. Pet. Geol. Bull., 65, 1617-1620, 1981.

Chase, C. G., and T. H. Gilmer, Precambrian plate tectonics: The midcontinent gravity high, Earth Planet. Sci. Lett., 21, 70-78, 1973.

Christie, P. A. F., V. J. Hughes, and B. L. N. Kennett, Velocity filtering of seismic reflection data, First Break, 1(3), 9-24, 1983.

Craddock, C., Late Precambrian regional geologic setting, in Geology of Minnesota: A Centennial Volume, edited by P. K. Sims and G. B. Morey, pp. 281-291, Minnesota Geological Survey, St. Paul, 1972.

Daniels, P. A., Jr., Upper Precambrian sedimentary rocks: Oronto group,Michigan-Wisconsin, Geology and Tectonics of the Lake Superior Basin, edited by R. J. Wold, and W. J. Hinze, Mem. Geol. Soc. Am., 156, 107-133, 1982.

Dix, C. H., Seismic velocities from surface measurements, Geophysics, 20, 68-86, 1955.

Dobrin, M. B., Introduction to Geophysical Prospecting, McGraw-Hill, New York, 1976.

Ells, G. D., Architecture of the Michigan Basin, in Studies of the Precambrian of the Michigan Basin, 1969 Annual Field Excursion, edited by H. B. Stonehouse, pp. 60-88, Michigan Basin Geological Society, Lansing, 1969.

Fowler, J. H., and W. D. Kuenzi, Keweenawan turbidites in Michigan (deep borehole red beds): A foundered basin sequence developed during evolution of a protoceanic rift system, J. Geophys. Res., 83, 5833-5843, 1978.

Green, J. C., Geology of Keweenawan extrusive rocks, Geology and Tectonics of the Lake Superior Basin, edited by R. J. Wold, and W. J. Hinze, Mem. Geol. Soc. Am., 156, 47-55, 1982.

Hall, H. C., The late Precambrian central North American rift system--A survey of recent geological and geophysical investigations, in Tectonics and geophysics of continental rifts, p. 111-123, NATO Adv. Stud. Inst. Ser. C, Vol. 37, edited by I. B. Ramberg and E.-R. Neumann, D. Reidel Hingham, Mass. 1978.

Hall, H. C., Crustal thickness in the Lake Superior region, in Geology and Tectonics of the Lake Superior Basin, edited by R. J. Wold, and W. J. Hinze, Mem. Geol. Soc. Am., 156, 239-243, 1982.

Haxby, W. F., D. L. Turcotte, and J. M. Bird, Thermal and mechanical evolution of the Michigan Basin, Tectonophysics, 36, 57-75, 1976.

Hinze, W. J., and D. W. Merritt, Basement rocks of the southern peninsula of Michigan, in Studies of the Precambrian of the Michigan Basin, 1969 Annual Field Excursion, edited by H. B. Stonehouse, pp. 28-59, Michigan Basin Geological Society, Lansing, 1969.

Hinze, W. J., R. L. Kellogg, and D. W. Merritt, Gravity and aeromagnetic anomaly maps of the southern peninsula of Michigan, Rep. Invest. 14, Geol. Surv. Div., Mich. Dep. of Nat. Resour., Lansing, 1971.

Hinze, W. J., R. F. Roy, and D. W. Davidson, The origin of Late Precambrian rifts, Geol. Soc. Am. Abstr. Programs, 4, 723, 1972.

Hinze, W. J., R. L. Kellogg, and N. W. O'Hara, Geophysical studies of basement geology of southern peninsula of Michigan, Am. Assoc. Pet. Geol. Bull., 59, 1562-1584, 1975.

Hinze, W. J., J. W. Bradley, and A. R. Brown, Gravimeter survey in the Michigan Basin deep borehole, J. Geophys. Res., 83, 5864-5868, 1978.

Hinze, W. J., R. J. Wold, and N. W. O'Hara, Gravity and magnetic anomaly studies of Lake Superior, Geology and Tectonics of the Lake Superior Basin, edited by R. J. Wold, and W. J. Hinze, Mem. Geol. Soc. Am., 156, 203-221, 1982.

Hoffman, P., Evolution of an early Proterozoic continental margin: The Coronation geosyncline and associated aulacogens of the northwestern Canadian shield, Philos. Trans. R. Soc. London, Ser. A,273, 547-581, 1973.

Kalliokoski, J., Jacobsville sandstone, Geology and Tectonics of the Lake Superior Basin, edited by R. J. Wold, and W. J. Hinze, Mem. Geol. Soc. Am., 156, 147-155, 1982.

Kennett, B. L. N., A comparison of travel-time inversions, Geophys. J. R. Astron. Soc., 44, 517-536, 1976.

Kin, A. R., and C. A. Jacewitz, Interactive model based weathering corrections, paper presented at 54th Annual International SEG meeting, Soc. of Explor. Geophys., Atlanta, GA, Dec. 2-6, 1984.

Landes, K. K., Petroleum Geology of the United States, pp. 75-84, John Wiley, New York,1970.

Lindseth, R. O., Digital Processing of Geophysical Data--A Review, Society of Exploration Geologists, Calgary, 1978.

Liu, C.-S., T. Zhu, H. Farmer, and L. Brown, An expanding spread experiment during COCORP field operation in Utah, in Reflection Seismology and the Continental Crust: A Global Perspective, Geodyn. Ser., vol. 13, edited by M. Barazangi and L. Brown, pp. 237-246, Washington, D.C., 1986.

March, D. W., and A. D. Bailey, A review of the two-dimensional transform and its use in seismic processing, First Break, 1(1), 9-21,1983.

McCallister, R. H., N. Z. Boctor, and W. J. Hinze, Petrology of the spilitic rocks from the Michigan Basin deep drill hole, J. Geophys. Res., 83, 5825-5831, 1978.

McClintock, P. L., Seismic data processing techniques for the northern Michigan reefs, paper presented at the Eastern Section Meeting, Am. Assoc. of Pet. Geol., East Lansing, Mich., Oct. 5-7, 1975.

Merk, G. P., and M. A. Jirsa, Provenance and tectonic significance of the Keweenawan interflow sedimentary rocks, Geology and Tectonics of the Lake Superior Basin, edited by R. J. Wold, and W. J. Hinze, Mem. Geol. Soc. Am., 156, 97-105, 1982.

Morey, G. B., and R. W. Ojakangas, Keweenawan sedimentary rocks of eastern Minnesota and northwestern Wisconsin, Geology and Tectonics of the Lake Superior Basin, edited by R. J. Wold, and W. J. Hinze, Mem. Geol. Soc. Am., 156, 135-146, 1982.

Nunn, J. A., and N. H. Sleep, Thermal contraction and flexure of intracratonal basin: a three-dimensional study of the Michigan Basin, Geophys. J. R. Astron. Soc., 76, 587-635,1984.

Ojakangas, R. W., and G. B. Morey, Keweenawan sedimentary rocks of the Lake Superior region: A summary, Geology and Tectonics of the Lake Superior Basin, edited by R. J. Wold, and W. J. Hinze, Mem. Geol. Soc. Am., 156,157-164,1982a.

Ojakangas, R. W., and G. B. Morey, Keweenawan pre-volcanic quartz sandstones and related rocks of the Lake Superior region, Geology and Tectonics of the Lake Superior Basin, edited by R. J. Wold, and W. J. Hinze, Mem. Geol. Soc. Am., 156, 85-96, 1982b.

Oliver, J., Exploration of the continental basement by seismic reflection profiling, Nature, 275, 485-488, 1978.

Robinson, E. A., and S. Treitel, Geophysical Signal Analysis, Prentice-Hall, Englewood Cliffs, N. J., 1980.

Sangree, J. B., and J. M. Widmier, Seismic interpretation of clastic depositional facies, in Seismic stratigraphy--Applications to hydrocarbon exploration, edited by C. E. Payton, Mem. Am. Assoc. Pet. Geol., 26, 165-184, 1977.

Serpa, L., T. Setzer, H. Farmer, L. Brown, J. Oliver, S. Kaufman, J. Sharp, and D. W. Steeples, Structure of the southern Keweenawan rift from COCORP surveys across the Midcontinent Geophysical Anomaly in northeastern Kansas, Tectonics, 3, 367-384,1984.

Sheriff, R. E., and L. P. Geldart, Exploration Seismology, vol. 2, Data-Processing and Interpretation, Cambridge University Press, Cambridge, 1983.

Sleep, N. H., and L. L. Sloss, A deep borehole in the Michigan Basin, J. Geophys. Res., 83, 5815-5819, 1978.

Sleep, N. H., and N. S. Snell, Thermal contraction and flexure of mid-continent and Atlantic marginal basins, Geophys. J. R. Astron. Soc., 45, 125-154, 1976.

Smith, T. J., J. S. Steinhart, and L. T. Aldrich, Crustal structure under Lake Superior, in The Earth Beneath the Continents, Geophys. Monogr. Ser., vol. 10, edited by J. S. Steinhart and T. J. Smith, pp. 181-197, AGU, Washington, D.C., 1966.

Steiner, D. R., On the velocity resolution of deep seismic reflection surveys, Master thesis, Cornell Univ., Ithaca, N. Y., 1984.

Taner, M. T., and F. Koehler, Velocity spectra--Digital computer derivation and applications of velocity functions, Geophysics, 34, 859-881, 1969.

Taner, M. T., F. Kochler, and K. A. Alhilali, Estimation and correction of near-surface time anomalies, Geophysics, 39, 441-463, 1974.

Watts, D. R., Paleomagnetism of the Fond Du Lac formation and the Eileen and Middle River sections with implication for Keweenawan tectonics and Grenville problem, Can. J. Earth Sci., 18, 829-841, 1981.

Weiblen, P. W., Keweenawan intrusive igneous rocks, Geology and Tectonics of the Lake Superior Basin, edited by R. J. Wold, and W. J. Hinze, Mem. Geol. Soc. Am., 156, 57-82, 1982.

White, W. S., Geologic evidence for crustal structure in the western Lake Superior Basin, in The Earth Beneath the Continents, Geophys. Monogr. Ser., vol. 10, edited by J. S. Steinhart and T. J. Smith, pp. 28-41, AGU, Washington, D.C., 1966.

Woollard, G. P., and H. R. Joesting, Bouguer anomaly map of the United States, AGU, Washington, D. C., 1964.

Zhu, T., and L. D. Brown, Two-dimensional velocity inversion and synthetic seismogram computation, Geophysics, in press, 1986.

L. D. Brown, INSTOC, Snee Hall, Cornell University, Ithaca, NY 14853.

T. Zhu, Tennessee Earthquake Information Center, Memphis State University, Memphis, TN 38152.

(Received April 14, 1986;
revised June 13, 1986;
accepted June 23, 1986.)